



LIGHTWEIGHT-FOCUSED STRUCTURAL OPTIMIZATION OF A TROLLEYBUS MOTOR MOUNTING BRACKET USING A TAGUCHI-FEM APPROACH

Ahmet ÖZCAN

Ulaşım İç ve Dış Ticaret A.Ş., R&D Center, Bursa, Türkiye, ahmet.ozcan@ulasim-as.com

Article Info

Received: December 9, 2025

Revised: January 14, 2026

Accepted: February 13, 2026

Keywords

*Lightweight Design,
Taguchi Method,
Finite Element Analysis,
Structural Optimization,
Motor Mounting Bracket,
Trolleybus,*

ABSTRACT

The increasing use of electric buses and trolleybuses in urban transportation requires the redesign of local structural components to achieve both lightweight performance and structural durability. In this context, the present study investigates the structural behavior and sheet-thickness optimization of a motor mounting bracket for a 12-m trolleybus using a combination of the Taguchi L9 orthogonal design method and finite element simulations. The analyses were conducted under quasi-static loading conditions assuming linear elastic material behavior, and boundary conditions representing the reaction forces transmitted from the traction motor to the chassis. Three geometric design parameters base sheet thickness, side sheet thickness, and stiffener sheet thickness were examined at three levels. Equivalent stress, displacement, safety factor, and mass were evaluated as response parameters, and the S/N ratio and ANOVA techniques were used to quantify parameter sensitivity and contribution to the variance of the mass response.

The results indicate that the base sheet thickness is the dominant parameter governing the lightweighting performance of the bracket, while the side and stiffener sheets have comparatively lower influence. The optimum thickness configuration was identified as 5–4–5 mm, yielding a 15.5% mass reduction with respect to the 6–6–5 mm reference design while maintaining a safety factor above 3.18. The findings demonstrate that the Taguchi-ANOVA-FEM approach provides an effective decision-support framework for early-stage design of bracket-type structural components in electric bus traction systems. Moreover, the methodology is compatible with manufacturable design constraints and can be extended to multi-objective formulations including durability and fatigue performance in future studies.

1. INTRODUCTION

The increasing use of electric buses and trolleybuses in urban public transportation necessitates the reconsideration of load-bearing body structures and auxiliary structural components in terms of both lightweight performance and structural strength. The integration of additional components such as battery packs, power electronics units, and traction motors increases the mass of the load-carrying structure and leads to elevated local stress levels. This situation has become a critical design parameter in terms of both energy consumption and operating costs. In recent years, studies focusing on the lightweighting of bus body and chassis structures and the enhancement of their structural performance have demonstrated that meaningful mass reductions can be achieved through the combined use of finite element analysis (FEA) and optimization methods. In the study conducted by Özcan et al. on a 25-m-long bi-articulated electric bus body, topology and size optimization were applied based on an experimentally validated finite element model derived from road test data, and approximately 14% mass reduction was achieved while preserving strength criteria [1]. Similarly, FEM-based investigations on the body and chassis stiffness, stress distributions, and fatigue life of mid- and large-sized buses have reported improvements in both mass and structural performance through the use of optimum cross-

section and sheet thickness combinations [2–4]. Moreover, studies examining the effects of power battery packs on body stiffness, natural frequencies, and stress distributions in electric vehicles have emphasized that additional mass can cause significant stress concentrations on local load-bearing components [5].

In addition to these full-scale body or chassis-level investigations, the structural performance of local components that directly affect the overall durability and operational safety of the vehicle—particularly connection and load-carrying brackets—has emerged as a distinct research area in recent years. In studies where the fatigue life of battery carrier brackets under random vibration loads was predicted using finite element analysis, it has been demonstrated that stress concentrations constitute the primary mechanism governing fatigue damage and that the fatigue performance can be improved through geometric optimization of the bracket [6]. In another study, the fatigue lives of two different bracket designs used in the charging door mechanism of an M3-class electric bus were investigated under constant-amplitude load cycles derived from real service data. The results, obtained by combining equivalent stress distributions and S–N curve-based life predictions, revealed that both material selection and geometric differences play a decisive role in fatigue safety [7]. For motor and transmission mounting brackets carrying powertrain components, finite element models are commonly calibrated with experimental test data, allowing fatigue life assessment to be performed prior to defining structural optimization-oriented design revisions [8]. In a recent study on upper brackets positioned on an automotive front-end frame, multi-objective optimization was applied under combined static and dynamic loading conditions, enabling both mass reduction and stiffness enhancement to be achieved simultaneously [9]. These findings indicate that bracket-type local components, although inseparable from the global body design, possess a significant independent potential for lightweighting and strength optimization.

In finite element-based structural design studies, the use of design of experiments (DOE) and statistical analysis methods for the systematic scanning of design parameters and the determination of optimum design combinations has become increasingly widespread. In particular, the Taguchi method is frequently preferred in the optimization of automotive structural components due to its ability to evaluate the effects of parameter levels on the response with a limited number of experiments or analyses, to assess performance robustness through signal-to-noise (S/N) ratios, and to quantify factor contributions via analysis of variance (ANOVA). Studies aiming to reduce the mass of automotive load-carrying elements using FEM-based Taguchi approaches have demonstrated that design variables such as sheet thickness can be optimized under safety factor and maximum stress constraints in chassis and structural members [10]. In a different study, the geometry of a single right-angle bracket was optimized under random vibration loads using a Taguchi L9 orthogonal array and the finite element method; the results showed that relatively small variations in bracket dimensions can lead to significant improvements in fatigue life [11-13]

In parameter optimization applications employing FEM–DOE/Taguchi hybrid models for truck and bus chassis structures, the effects of geometric variables such as thickness and cross-section dimensions on mass, maximum stress, and safety factor have been statistically evaluated, and balanced design solutions between minimum mass and allowable stress levels have been reported [10,14,15]. Barea et al. (2018) demonstrated that design parameters have pronounced effects on fatigue behavior and structural performance in their Taguchi-based optimization study on a right-angle bracket [11]. Similarly, Patel and Bhatt (2016) reported that an FEM–Taguchi-based optimization process provides a feasible approach for improving mass and performance outputs in heavy vehicle chassis components [16]. The 15.5% mass reduction achieved in the present study is consistent with the optimization trends reported in the Taguchi–FEM literature and supports the engineering tendency toward lightweighting of structural bracket designs in heavy commercial vehicles. Furthermore, studies integrating random vibration fatigue analysis with design optimization for bracket-like components subjected to heavy-duty service conditions, such as energy storage enclosures and battery housings, have demonstrated that FEM-based design–experiment integration is an effective tool for developing reliable and lightweight structures [10].

The collective findings in the literature indicate that: (i) FEM-based lightweighting and structural performance assessment has become widespread in bus bodies and heavy commercial vehicle chassis

structures, (ii) local components such as battery, charging door, and powertrain brackets are critical in terms of static and fatigue strength, and (iii) the FEM–Taguchi integration provides a suitable framework for the systematic optimization of sheet thickness and geometric parameters. However, no study has been identified in which the sheet thickness parameters of the main motor mounting bracket in trolleybus applications have been systematically investigated using a Taguchi experimental design and in which the interaction between mass, safety factor, and displacement has been evaluated in a comprehensive manner.

The original contribution of the present study is to systematically scan three fundamental sheet thickness parameters namely the base plate, side plates, and intermediate stiffener plate of a motor mounting bracket belonging to a 12-m-long trolleybus using a Taguchi L9 orthogonal array. For each design combination, the maximum equivalent stress, displacement, safety factor, and total mass are computed through finite element analysis, and the optimum thickness combination is determined within a lightweight-focused performance framework. By employing S/N ratios and ANOVA results, the relative effects of the design parameters on mass are quantitatively revealed, and the base plate thickness is demonstrated to be the dominant design variable in terms of lightweighting performance. Consequently, a motor mounting bracket design is proposed for the trolleybus traction system that satisfies structural safety requirements while providing a meaningful level of mass reduction compared to the reference design.

2. MATERIAL AND METHOD

2.1. Bracket Geometry and Material Properties

The detailed geometry of the bracket is illustrated in Figure 1. The bracket has an overall width of 412 mm and a height of 158 mm in the initial configuration. The intermediate stiffener divides the structure into two sub-sections of 220 mm and 192 mm, respectively. The mounting interfaces are realized through two cylindrical features, with inner and outer radii of 30 mm and 40 mm. A top-view representation shows that the plate thickness of all structural members is 6 mm. In addition, the support plates forming the lateral load path are dimensioned as 140 mm × 158 mm and 180 mm × 120 mm, with a 20 mm connecting flange. These geometric definitions characterize the design envelope of the bracket and define the available space for motor mounting and chassis integration.

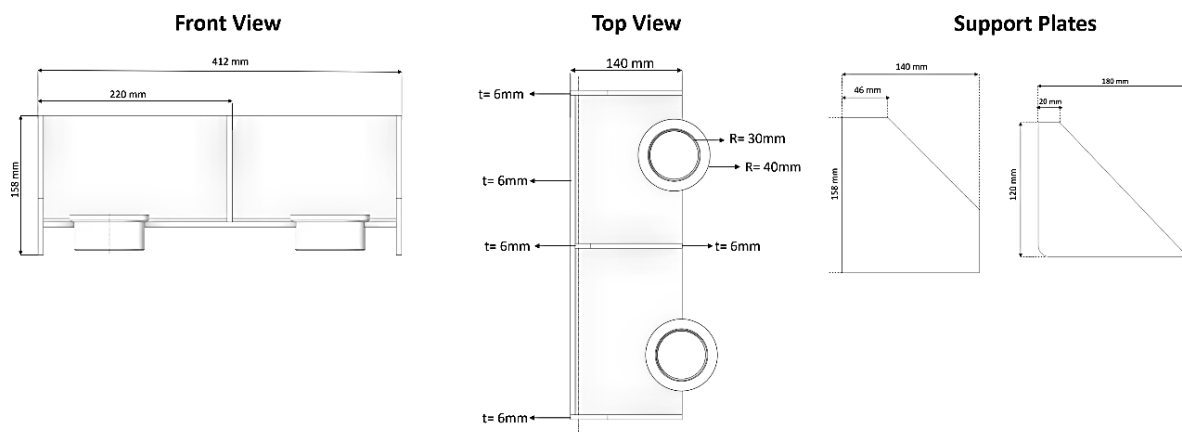


Figure 1. Dimensional representation of the motor mounting bracket with geometric constraints and support plate configuration

The bracket is manufactured from a low-carbon structural steel with mechanical properties equivalent to the EN 10025-2 grade S355J2. In the context of the present study, this material can be regarded as approximately corresponding to an AISI 10xx-series structural steel (similar to AISI 1024), with a minimum yield strength of about 355 MPa and a tensile strength in the range of 510–630 MPa. The mechanical properties used in the analyses are summarized in Table 1.

Table 1. Mechanical properties of the bracket material (EN 10025-2 S355J2, approx. AISI 10xx structural steel) [17],[18]

Parameters	Value
Density g/cm ³	7.85
Elastic Modulus (GPa)	210
Poisson's Ratio (ν)	0.3
Yield Strength (MPa)	355-420
Tensile Strength (MPa)	490-630
Shear Modulus (GPa)	81
Elongation (%)	20-24

The bracket was manufactured from a structural steel equivalent to EN 10025-2 grade S355J2 due to its favorable balance between stiffness, yield strength, fatigue resistance and manufacturability. In heavy-duty commercial platforms such as trolleybuses, the mounting components of traction motors are subjected to repeated load cycles during acceleration and braking, making low-carbon structural steels more suitable than aluminum alloys or composite laminates, which offer higher specific strength but may exhibit reduced fatigue robustness and impose limitations in welding and joining operations. S355-class steels are also widely available in flat sheet stock, compatible with MAG/MIG welding processes, and cost-effective for mass production, which makes them industrially preferred for bracket and mounting assemblies. The material choice is consistent with the literature, where sheet-metal brackets and metallic support components are frequently adopted for chassis-mounted or load-transfer structural applications in automotive platforms [19–21].

2.2. Finite Element Model of the Bracket

2.2.1. FEM Literature Context

Finite element-based methodologies are widely employed in the assessment of sheet-metal brackets and structural components due to their capability of capturing bending-dominated deformation modes and localized stress concentrations with high numerical fidelity. In the literature, shell-element formulations have been extensively used for thin-walled structures, as they allow for accurate prediction of equivalent stress distributions at a reduced computational cost [20–22]. Moreover, hybrid meshing strategies combining shell and solid elements have been reported to improve stress resolution in load-transfer regions of mounting assemblies and bolted or welded joints [23–25]. For motor mounts and support brackets subjected to quasi-static loads, linear elastic FEM approaches have demonstrated sufficient accuracy for the preliminary evaluation of structural rigidity and strength, especially in the early design stages [26,28]. The finite element modeling approach followed in this study is consistent with these previous findings and tailored to the geometric characteristics of the proposed bracket.

2.2.2. Mesh Characteristics

The finite element model of the motor mounting bracket was constructed using quadrilateral shell elements to accurately represent the bending-dominated behavior of the sheet-metal structure. During the mesh generation process, mesh independence and element size sensitivity were taken into account to ensure that the solution became independent of the spatial discretization [29]. Based on these evaluations, a nominal element size of 2 mm was selected as the optimal resolution in terms of computational efficiency and model accuracy. In regions subjected to localized load transfer, solid elements were employed and discretized using an orthogonal meshing strategy, as recommended in the literature for load-bearing plate and bracket analyses [30].

The final mesh consisted of 170,052 nodes and 137,498 elements, with an average element quality of 0.89. The predominance of quadrilateral shell elements ensured favorable accuracy in stress prediction and reduced numerical locking. A detailed view of the discretized mesh structure is provided in Figure 2.

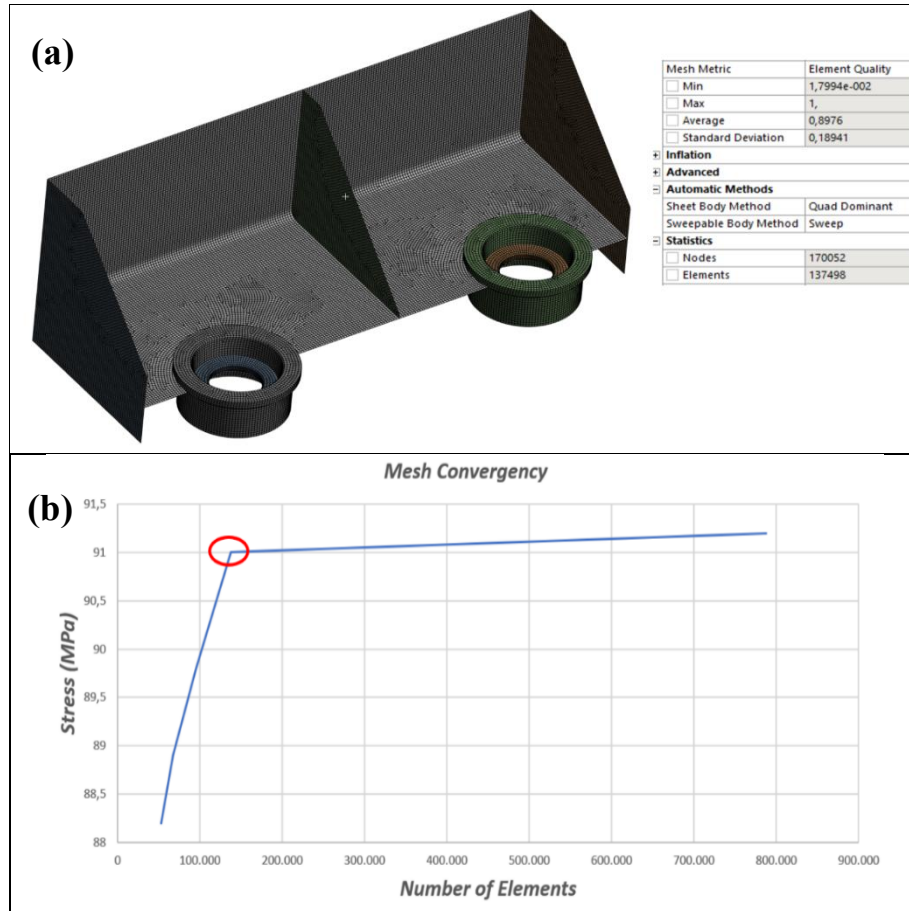


Figure 2. (a) Finite Element Mesh Structure, (b) Finite Element Convergence Plot

2.2.3. Finite Element Method

The Finite Element Method (FEM) is a numerical analysis technique used to determine, through approximate methods, the behavior of complex engineering geometries that cannot be solved analytically. The method is based on dividing the modeled structure into small elements and defining the displacement field within each element using local shape functions. Through this approach, stress, strain, and displacement distributions can be calculated by considering material properties, boundary conditions, and applied loads. Under the assumption of linear elasticity, FEM solves the structural equations using Hooke's law, force–displacement relationships, and the principle of energy equilibrium. In this study, the analyses were carried out using a linear static solution approach, and the stresses developed in the bracket were evaluated according to the von Mises criterion. The fundamental mathematical formulation of the finite element analysis is expressed in the following general form [18],[29]:

$$Ku = F \quad (1)$$

Here, K represents the global stiffness matrix, u denotes the nodal displacement vector, and F corresponds to the external load vector. The element stiffness matrix is obtained at the element level based on the principle of virtual work and is expressed as follows [18],[29]:

$$K_e = \int_V B^T D B dV \quad (2)$$

In this equation, B represents the strain–displacement matrix derived from the shape functions, and D denotes the material-dependent elasticity matrix. The von Mises equivalent stress, which was taken as the reference parameter for the safety evaluation of the bracket design, is calculated using the following expression [18],[29]:

$$\sigma_{eq} = \sqrt{\frac{1}{2}[(\sigma_1 - \sigma_2)^2 + (\sigma_2 - \sigma_3)^2 + (\sigma_3 - \sigma_1)^2]} \quad (3)$$

This formulation enables complex multi-axial stress states to be represented by a single scalar quantity, thereby allowing direct comparison in engineering design. The analysis results obtained based on this method were evaluated together with the Taguchi method to establish the optimum design decisions.

2.3. Boundary Conditions and Load Application

The loading acting on the bracket was applied through the mounting interfaces illustrated in Figure 3. For the static analyses, the traction motor mass was assumed to be 400 kg and considered under standard gravitational loading (1 g), corresponding to a downward force of approximately 3922 N. The load was uniformly distributed over the contact surface to prevent numerical singularities and to ensure realistic load transfer at the mounting interface.

The welded faces connecting the bracket to the vehicle chassis were modeled as fully constrained, restricting all translational and rotational degrees of freedom ($U_X = U_Y = U_Z = ROT_X = ROT_Y = ROT_Z = 0$). No contact non-linearity was considered in the interface regions, and the chassis connection was treated as rigid to represent the high stiffness of the welded joints.

A linear static structural analysis was performed under small-deformation and isotropic elasticity assumptions. Further details regarding the mesh configuration and finite element methodology are provided in Section 2.2.1 and 2.2.2.

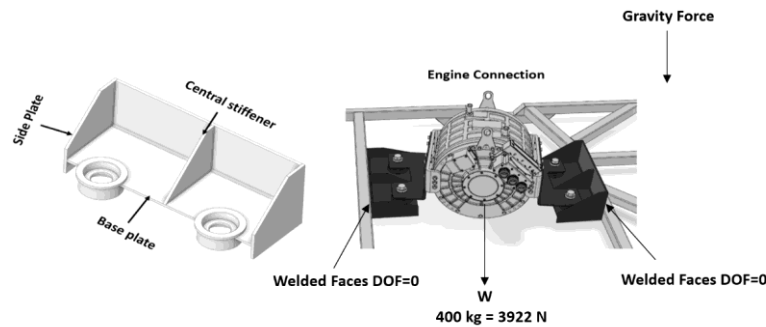


Figure 3. Motor mounting bracket connection showing load application and boundary conditions.

The numerical model was verified through a mesh independence study and numerical consistency checks to ensure that the finite element solution was not sensitive to spatial discretization. The structural responses obtained for the reference 6–6–5 configuration were found to be consistent with the stiffness and stress levels typically reported for sheet-metal brackets and mounting assemblies in the literature. In addition, the deformation modes observed in the analyses exhibited the global bending behavior expected for base-plate-dominated geometries, confirming that the load-transfer mechanisms were physically meaningful. Although experimental validation is beyond the scope of the present study, the adopted verification and benchmarking steps provide sufficient confidence in the model accuracy for the screening-level design evaluation carried out in this work.

In the finite element simulations, the material behavior was assumed to be linear elastic and isotropic due to the quasi-static nature of the applied loading. The traction motor was represented by an equivalent static load acting on the mounting interface, and the effects of dynamic excitation, damping, temperature variation and manufacturing tolerances were neglected. The simulations were carried out under standard gravitational acceleration and were limited to the evaluation of structural stiffness and strength. The boundary conditions were defined to represent the reaction forces transmitted from the vehicle chassis to the bracket, and no relative motion was allowed at the bolted interfaces. These assumptions are considered reasonable for early-stage structural screening and optimization studies.

2.4. Taguchi Experimental Design

The Taguchi method is a systematic experimental design approach that enables the determination of parameter effects with a limited number of experiments [31,32]. In this study, a Taguchi-based experimental design was applied in order to systematically investigate the main geometric parameters affecting the structural behavior of the motor mounting brackets. Three different design factors were defined, each at three levels: (i) base plate thickness, (ii) side plate thickness, and (iii) central stiffener thickness. These factors were selected because of their direct influence on bracket stiffness, load transfer capacity, and stress distribution. The Taguchi L9 orthogonal array was used to generate the experimental combinations, thereby providing a representative sampling of the design parameter space with a minimum number of analyses. Within the L9 layout, nine different thickness combinations were evaluated, with each row representing a distinct design configuration in the finite element analyses. This approach enables both the systematic evaluation of the sensitivity of the load path to thickness parameters and the statistical identification of the dominant factor levels affecting structural performance during the optimization process.

In this study, a parameter space consisting of three design factors, each with three different thickness levels, was defined. Using the L9 orthogonal array structure of the Taguchi method, nine experimental combinations were generated, and each combination was modeled as a distinct design variant evaluated through finite element analysis. The design factors and their corresponding levels used in the study are presented in Table 2.

Table 2. Experimental combinations and factor levels used in the Taguchi L9 orthogonal design

Factor	Description	Level 1	Level 2	Level 3
A	Base plate thickness (mm)	4	5	6
B	Side plate thickness (mm)	4	5	6
C	Central stiffener thickness (mm)	4	5	6

The experimental combinations generated according to the factor levels are presented in Table 3.

Table 3. Experimental combinations used in the Taguchi L9 orthogonal design

Experiment No	A – Base Plate (mm)	B – Side Plate (mm)	C – Stiffener Plate (mm)
1	4	4	4
2	4	5	5
3	4	6	6
4	5	4	5
5	5	5	6
6	5	6	4
7	6	4	6
8	6	5	4
9	6	6	6

This design structure provides the statistical basis for determining the optimum factor levels according to the mass response obtained from the finite element analysis.

2.5. S/N Calculation Method

Within the scope of the Taguchi method, signal-to-noise (S/N) ratios were calculated in order to evaluate the performance sensitivity of the experimental results. In this study, the “smaller-the-better” approach was selected as the optimization criterion, and the S/N ratio was calculated using Equation (4). For comparative cases, the “larger-the-better” approach is presented in Equation [30-33] (5).

$$S/N = -10 \log \left(\frac{1}{n} \sum_{i=1}^n y_i^2 \right) \tag{4}$$

$$S/N = -10 \log \left(\frac{1}{n} \sum_{i=1}^n \frac{1}{y_i^2} \right) \quad (5)$$

In this study, since lightweighting is the primary objective, the “smaller-the-better” approach, which directly rewards the minimization of the performance output represented by mass, was adopted. This approach is widely preferred in the literature for Taguchi-based studies focused on weight optimization [33].

2.6. Anova Analysis

In this study, a one-way analysis of variance (ANOVA) was applied in order to statistically evaluate the effects of the design parameters on the total mass of the bracket. ANOVA makes it possible to determine the relative influence of each design factor on the final response and to quantify the proportion of variance explained in the response variable. The analysis results obtained within the scope of the Taguchi experimental design were evaluated based on contribution ratios and F-values, and thus the level of influence of the design parameters on the performance response was quantitatively determined in a statistical manner. This method provides a basis for systematically improving the design variables by identifying the parameters that play a dominant role in the optimization process. Through the use of ANOVA, the relative effects of the design parameters on the response were quantitatively determined.

Table 4. Results of the variance analysis (ANOVA) performed for the bracket mass

Factor	SS (Sum of Squares)	DOF	MS	F-Value	Contribution (%)
A (Base plate thickness)	10.8610	2	5.4305	719.80	87
B (Side plate thickness)	1.5551	2	0.7775	103.06	12.5
C (Central stiffener thickness)	0.0524	2	0.0262	3.47	0.4
Error	0.0151	2	0.0075	-	0.1
Total	12.4835	8	-	-	100

The results of the variance analysis (ANOVA) performed for the bracket mass are presented in Table 4. According to the results, the base plate thickness is observed to be the most dominant design factor by explaining 87.0% of the total variance. The side plate thickness ranks second with a contribution of 12.5%, while the effect of the central stiffener thickness is negligible.

3. RESULTS

In this section, the results obtained from the finite element analyses carried out within the scope of the Taguchi L9 experimental design are presented. For each design combination, the total mass of the bracket, maximum equivalent stress, maximum displacement, and the calculated safety factor were evaluated. These outputs were compared in accordance with the lightweighting criterion, and the optimum design level was determined by calculating the S/N ratios in accordance with the Taguchi method.

The finite element analysis results of the Taguchi experimental design are presented in Table 5.

Table 5. FEA results (stress/displacement/mass/safety factor for Trials 1–9)

Experiment No	A – Base Plate (mm)	B – Side Plate (mm)	C – Stiffener Plate (mm)	Equivalent Stress (MPa)	Displacement (mm)	Mass (kg)	Safety	Natural Frequency (Hz)
1	4	4	4	193	0.59	11.08	1.81	23.146
2	4	5	5	128	0.53	11.68	2.73	24.386
3	4	6	6	117	0.51	12.27	2.99	25.431
4	5	4	5	110	0.36	12.61	3.18	29.252
5	5	5	6	88	0.32	13.22	3.97	30.59
6	5	6	4	80	0.31	13.41	4.37	30.948
7	6	4	6	70	0.23	13.86	5	35.366
8	6	5	4	64	0.22	14.32	5.46	35.756
9	6	6	5	59	0.21	14.92	5.93	37.229

When Table 5 is examined, it is observed that although the increase in thickness levels reduces the equivalent stress and displacement, it leads to a significant increase in mass. Nevertheless, it is confirmed that the safety factor remains within the range of 1.81 to 5.93 for all design combinations and stays within safe design limits. This indicates that the design factors have a direct influence on both stiffness and lightweight performance.

In addition, it is observed that the natural frequency values increase with increasing thickness, and particularly that the 4–4–4 configuration exhibits values close to the resonance limits. This demonstrates that the modal performance is sensitive to the design variables and should be considered together with static optimization.

For the purpose of optimizing the bracket mass, S/N ratios were calculated for each experimental combination using the “smaller-the-better” approach. The calculated values are presented in Table 6.

Table 6. S/N Values

Experiment No	Mass (kg)	S/N(dB)
1	11.08	-20.89
2	11.68	-21.35
3	12.27	-21.78
4	12.61	-22.01
5	13.22	-22.42
6	13.41	-22.55
7	13.86	-22.84
8	14.32	-23.12
9	14.92	-23.48

When the S/N values given in Table 6 are examined, according to the “smaller-the-better” criterion, a decrease in the absolute value of the S/N ratio—that is, the value approaching zero—is considered to represent better performance. In this regard, the highest S/N value of -20.89 dB was obtained in Trial 1, corresponding to the 4–4–4 mm thickness combination. As the thickness levels increase, the bracket mass increases in parallel, causing the S/N values to shift toward more negative levels. In particular, the fact that Trial 9, with the 6–6–5 mm combination, has the lowest S/N ratio (-23.48 dB) indicates that this configuration provides the poorest performance in terms of mass. These results reveal that the bracket mass is highly sensitive to the design factors and that an increase in thickness directly leads to performance degradation. Similar studies in the literature have shown that a significant degree of lightweighting can be achieved by reducing thickness in bracket components [11,29].

Using the S/N values obtained from the experiments, the level averages for each factor were calculated. This process allows the relative effects of the design variables on the response to be analyzed in a comparable manner. The calculated average S/N levels are presented in Table 7.

Table 7. Average S/N values of factor levels and the optimum design combination

Factor	Description	Level 1	Level 2	Level 3	Optimum Level
A	Base plate thickness (mm)	- 21.31 dB	-22.33 dB	-23.15 dB	A1 (4mm)
B	Side plate thickness (mm)	- 21.43 dB	-22.29 dB	-22.96 dB	B1 (4 mm)
C	Central stiffener thickness (mm)	- 21.56 dB	-22.25 dB	-22.87 dB	C1 (4mm)

When the average S/N values presented in Table 7 are examined, it is observed that the highest (least negative) S/N values for all design factors occur at the first level (4 mm). For the “smaller-the-better” criterion, a higher S/N ratio corresponds to a lower response (i.e., lower bracket mass) and therefore better performance. Accordingly, the optimum design combination is defined as A1–B1–C1, that is, the configuration in which the base plate, side plate, and central stiffener thicknesses are all 4 mm. This combination minimizes the total mass of the bracket within the investigated design space while maintaining acceptable structural strength.

When the main effects plot presented in Figure 4 is examined, it is observed that the S/N values shift toward more negative levels as the factor levels increase for all design factors, reflecting the increase in mass with thickness. For the “smaller-the-better” criterion, the optimum level is the one with the highest (least negative) S/N ratio; therefore, the optimum level for all factors is determined to be 4 mm. In addition, the comparison of the slopes reveals that the base plate thickness (Factor A) has the highest sensitivity on the S/N response, whereas the side plate thickness (Factor B) and the central stiffener thickness (Factor C) exhibit more limited effects. These results are consistent with the statistical findings obtained from the ANOVA analysis.

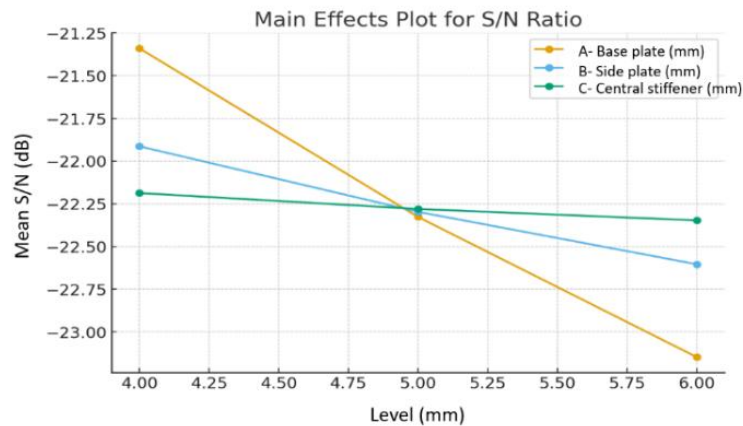
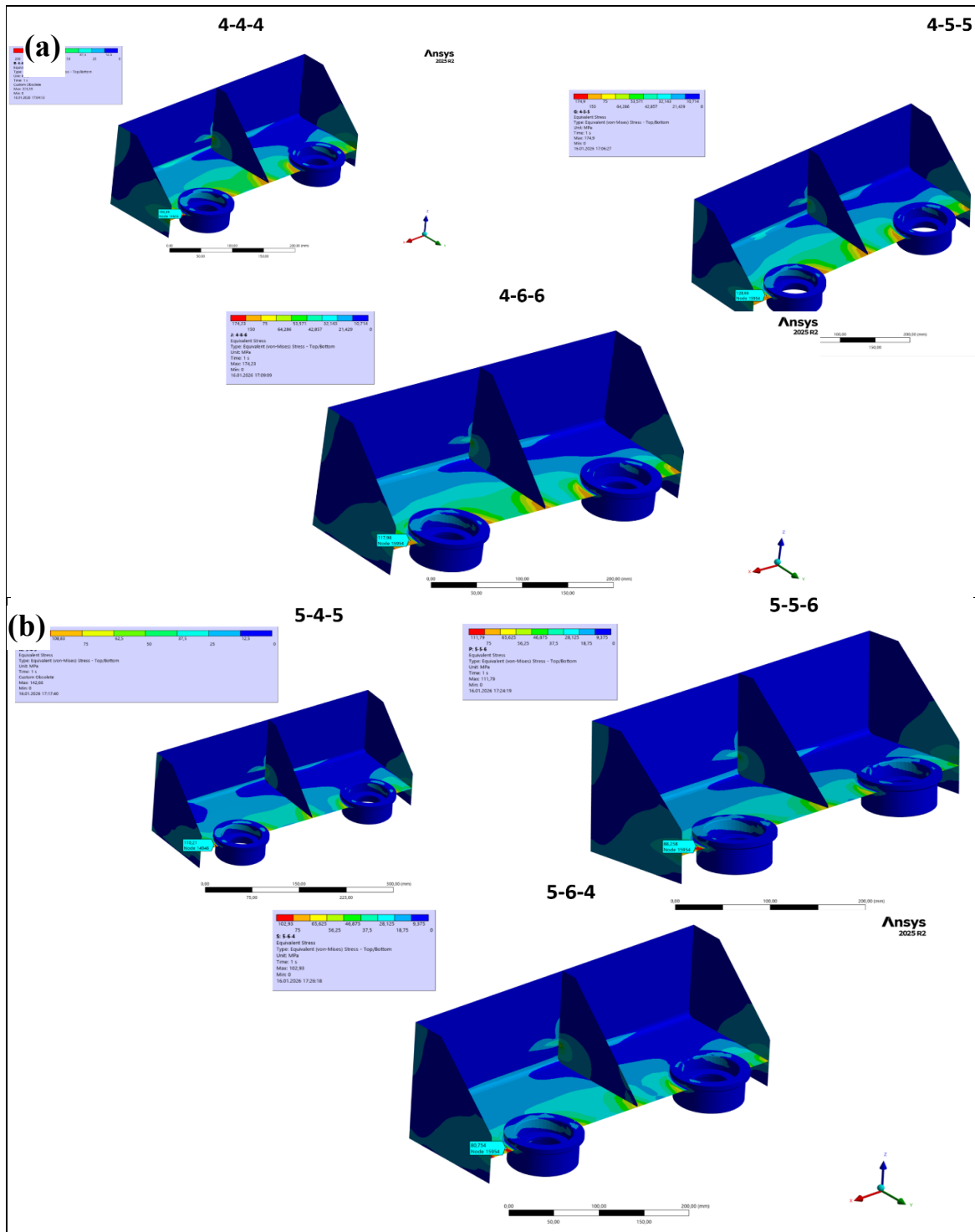


Figure 4. Taguchi Main Effects Plot (S/N graph)

The equivalent von Mises stress results obtained from the nine design configurations are summarized in Table 5 and presented in Figure 5 for direct visual comparison. Overall, the peak stress levels varied between 59 MPa and 193 MPa, while the corresponding factors of safety ranged from 1.81 to 5.93, highlighting the strong sensitivity of the bracket response to the sheet-thickness distribution. Among these configurations, the 4–4–4 and 4–5–5 thickness combinations exhibited the highest stress levels, corresponding to the lowest sheet-thickness values within the design space and therefore to the weakest stiffness contributions. In contrast, the 6–6–5 reference configuration generated the lowest stress values, as expected from the increased thickness of both the base and side sheets. The remaining configurations (5–4–4, 5–5–4 and 4–6–5) exhibited intermediate stress levels, reflecting varying contributions of the base, side and stiffener sheets to the load transfer behavior of the bracket. These results confirm the classical stiffness–mass trade-off characteristic of sheet-metal structural components, in which reduced thickness improves mass performance at the expense of stress intensification in critical load-bearing regions. Within this context, the 5–4–5 configuration was identified as a compromise solution between mass reduction and structural safety, yielding a peak von Mises stress of 110 MPa with a factor of safety of 3.18, while providing a 15.5% weight reduction compared to the initial bracket configuration.



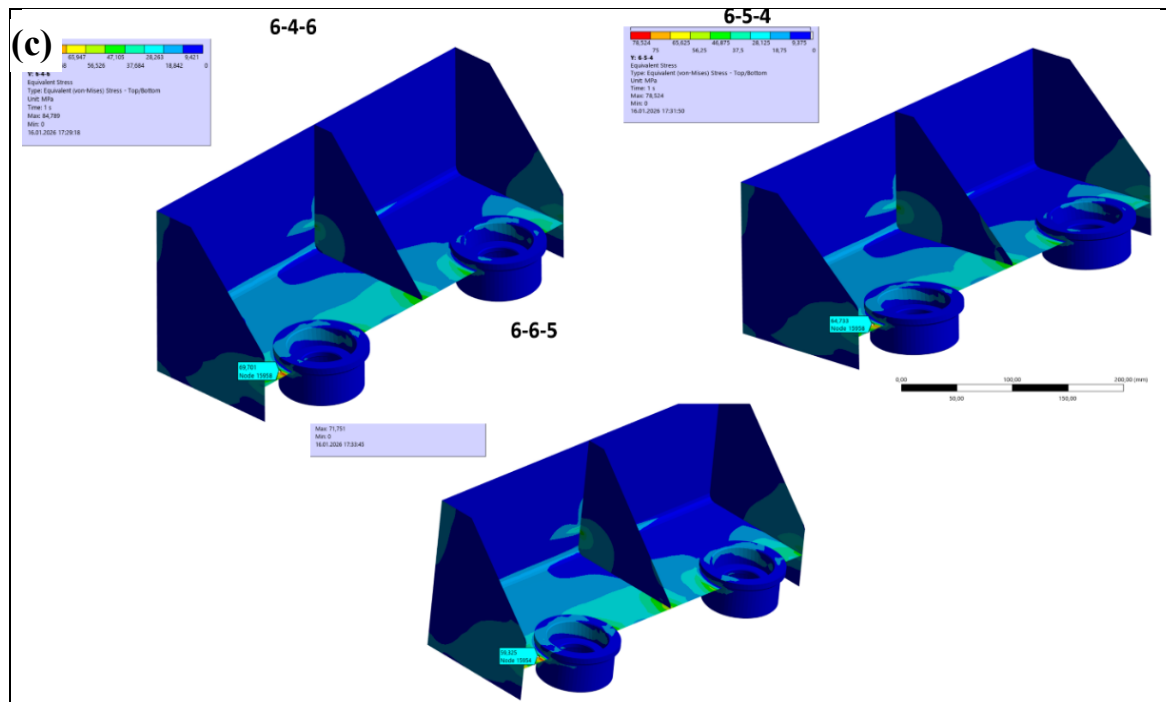


Figure 5. Equivalent von Mises stress comparison across the L9 Taguchi orthogonal-array design configurations, validating the selection of the optimal bracket thickness combination via finite element analysis.

Under identical loading and boundary conditions, the deformation patterns obtained from the reference (6–6–5), optimized (5–4–5), and extreme low-thickness (4–4–4) configurations exhibited similar global bending modes dominated by the base plate rigidity. However, a clear thickness-dependent deformation trend was observed. The maximum deformations were 0.21 mm for the reference 6–6–5 case, 0.36 mm for the 5–4–5 optimized configuration, and 0.59 mm for the 4–4–4 configuration. These results align with the stiffness–compliance behavior expected for sheet-metal assemblies, where thickness reduction improves mass performance at the expense of increased deformation. Despite its higher compliance relative to the reference case, the 5–4–5 configuration remained within acceptable engineering limits, validating it as a structurally feasible lightweight solution (Figure 6).

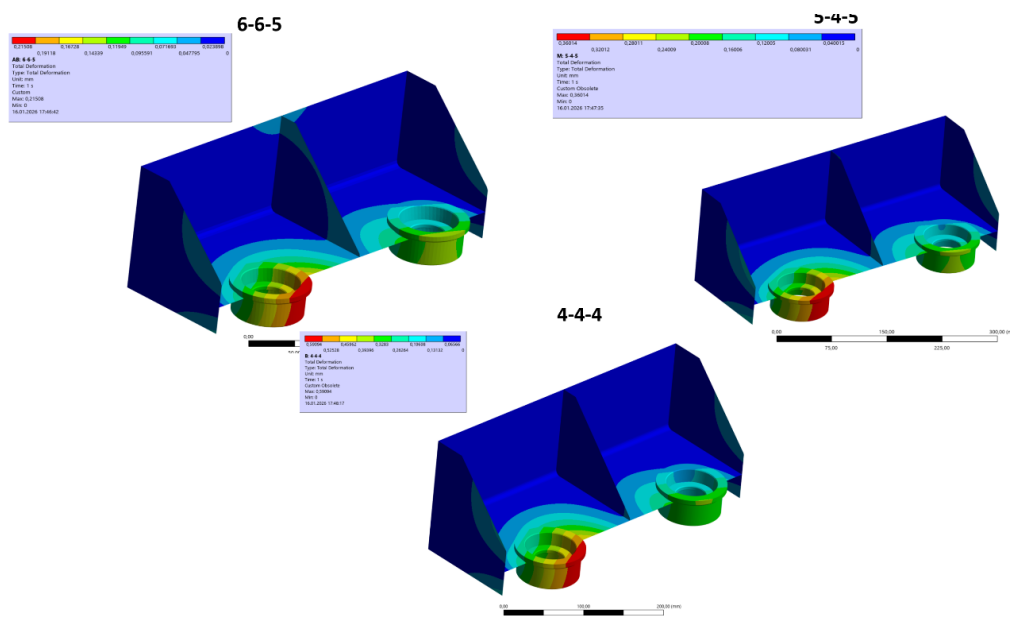


Figure 6. Comparison of total deformation responses for the 6–6–5, 5–4–5, and 4–4–4 design configurations obtained by finite element analysis.

4. DISCUSSION AND CONCLUSIONS

In this study, the structural behavior of a motor mounting bracket for an electric bus traction system was investigated through finite element simulations combined with a Taguchi-based design methodology. The results show that the primary load path is governed by the base sheet, which directly transfers reaction forces from the traction motor to the chassis. This finding is consistent with bracket and support optimization studies reporting that similar metallic components are dominated by their main load-carrying regions [19], [34].

The ANOVA results, in which the base factor accounts for the majority of the variance, agree with Taguchi-based DOE applications on L-brackets, sheet-metal supports and snap-fit assemblies, where a single geometric factor was shown to explain a dominant portion of the response variability [10], [19]-[21], [30], [35], [36]. This confirms that the Taguchi-ANOVA framework is suitable for sensitivity evaluation during early-stage design decisions.

From a lightweighting perspective, the optimum sheet configuration was identified as 5–4–5 mm, achieving approximately 15.5% mass reduction relative to the 6–6–5 mm reference, while maintaining a maximum equivalent stress below 110 MPa and a safety factor greater than 3.18. Comparable mass reductions (10–20%) have been reported in redesign studies on metallic brackets and support structures without compromising structural performance [20],[33], [34].

Modal analysis revealed increased global stiffness, shifting the first natural frequency outside the typical excitation band of traction motors. Similar modal improvements were observed in engine mounting bracket studies emphasizing resonance avoidance [27], [34].

A key implication of this work is that mass-based single-response optimization may lead to structurally insufficient designs, emphasizing the need to include criteria such as stress, displacement and fatigue. Limitations include linear static modeling assumptions, deterministic boundary conditions and discrete sheet-thickness levels. Future work will focus on multi-objective optimization and prototype-level validation under representative operating conditions.

Statement of Research and Publication Ethics

The study is complied with research and publication ethics.

Artificial Intelligence (AI) Contribution Statement

This manuscript was entirely written, edited, analyzed, and prepared without the assistance of any artificial intelligence (AI) tools. All content, including text, data analysis, and figures, was solely generated by the authors.

REFERENCES

- [1] A. Özcan, İ. Yönel, and C. Yüce, "Lightweight design and structural analysis of a bi-articulated bus: Experimental measurements and FEM validation," *Engineering Science and Technology, an International Journal*, vol. 70, p. 102169, 2025, doi: 10.1016/j.jestch.2025.102169.
- [2] N. T. Tam, T. P. Le, N. T. Huynh, and Q. M. Nguyen, "Optimization of frame structure coach 29/34 seats in static durability state," *Engineering Science and Technology, an International Journal*, vol. 47, p. 101523, 2023, doi: 10.1016/j.jestch.2023.101523.
- [3] A. Agarwal and L. Mthembu, "Structural analysis and optimization of heavy vehicle chassis using aluminium P100/6061 Al and Al GA 7-230 MMC," *Processes*, vol. 10, no. 2, p. 320, 2022, doi: 10.3390/pr10020320.
- [4] D. Crococolo, M. De Agostinis, and N. Vincenzi, "Structural analysis of an articulated urban bus chassis via FEM: A methodology applied to a case study," *Strojniški Vestnik – Journal of Mechanical Engineering*, vol. 57, no. 11, pp. 799–809, 2011, doi: 10.5545/sv-jme.2011.077.
- [5] K. Wang, P. Shi, and Z. Zhang, "Finite element modeling of electric vehicle power battery pack and its influence analysis and test research at body-in-white stage," *Journal of Vibroengineering*, vol. 25, no. 7, pp. 1353–1368, 2023, doi: 10.21595/jve.2023.23260.

- [6] M. Zhou, “The fatigue life analysis of the battery bracket,” in *Proc. Int. Conf. on Advances in Energy, Environment and Chemical Engineering (ICAEEES)*, Atlantis Press, 2015, doi: 10.2991/icaees-15.2015.136.
- [7] Karabulut, S., Özcan, A., & Inal, A. B. (2025). Fatigue life evaluation of a bus charging door bracket. *Pamukkale Üniversitesi Mühendislik Bilimleri Dergisi (Advanced Online Publication)*. <https://doi.org/10.5505/pajes.2025.61168>
- [8] E. Eryılmaz, *Development of Analysis Methodology for Engine Brackets*, Hexagon Studio Technical Report, 2016.
- [9] Z. Zhang, J. Liu, Y. Li, and X. Wang, “Structure optimisation research for the upper bracket of automobile front-end frame based on the compromise programming method,” *SN Applied Sciences*, vol. 7, no. 2, p. 196, 2025, doi: 10.1007/s42452-025-06727-6.
- [10] T. M. Patel and N. M. Bhatt, “FEM based Taguchi method to reduce the automobile structural member weight,” *GIT J. Eng. Technol.*, vol. 8, pp. 2–11, 2015.
- [11] R. Barea, S. Novoa, F. Herrera, B. Achiaga, and N. Candela, “A geometrical robust design using the Taguchi method: Application to a fatigue analysis of a right angle bracket,” *DYNA*, vol. 85, no. 205, pp. 37–46, 2018, doi: 10.15446/dyna.v85n205.67547.
- [12] M. S. Gümüş, M. Kalyoncu, and V. Alver, “Geometric optimization of a right-angle bracket to maximize fatigue life using Taguchi method,” in *Proc. Int. Conf. on Materials and Engineering Technology (ICMET)*, Gaziantep, Türkiye, Nov. 2020.
- [13] D. T. Giang, “Reasonable design method of box crane girder by Taguchi method,” *J. Appl. Eng. Sci.*, vol. 22, no. 1, pp. 100–112, 2024, doi: 10.5937/jaes0-45536.
- [14] D. Maheswara et al., “Multi-objective optimization of structural design for lightweight vehicle chassis using DoE, FEA and ANOVA,” *Automotive Experiences*, early access, 2025, doi: 10.31603/ae.13567.
- [15] T. M. Patel and N. M. Bhatt, “Parametric optimization of Eicher 11.10 chassis frame for weight reduction using FEA–DOE hybrid modeling,” *IOSR J. Mech. Civ. Eng.*, vol. 6, no. 2, pp. 92–100, 2013, doi: 10.9790/1684-06292100.
- [16] X. Hu, Y. Li, W. Zhang, and J. Zhang, “Fatigue analysis of an energy storage supercapacitor box under random vibration,” *Scientific Reports*, vol. 15, p. 92116, 2025, doi: 10.1038/s41598-025-92116-3.
- [17] *Hot Rolled Products of Structural Steels – Part 2: Technical Delivery Conditions for Non-Alloy Structural Steels*, EN 10025-2, European Standard, 2004.
- [18] R. D. Cook, D. S. Malkus, and M. E. Plesha, *Concepts and Applications of Finite Element Analysis*, 4th ed., New York, NY, USA: John Wiley & Sons, 2002.
- [19] S. F. Sakore and K. A. Mahajan, “Design of arm & L-bracket and its optimization by using Taguchi method,” *IOSR Journal of Mechanical and Civil Engineering*, vol. 17, no. 10, pp. 28–38, 2017, doi: 10.9790/1684-17010062838.
- [20] Guzmán-Siles et al., “Optimization of metallic support geometry for automotive doors using CAD, CAE, and Taguchi method to improve structural rigidity,” *Eng*, vol. 6, no. 12, p. 361, 2025, doi: 10.3390/eng6120361.
- [21] M. Prasad and A. Sai Kumar, “Topography optimization of sheet metal bracket using Taguchi’s design of experiments for varying materials and load conditions,” *International Journal of Research Publication and Reviews*, vol. 6, no. 1, pp. 2067–2075, 2025.
- [22] Bischoff, M., Wall, W. A., Bletzinger, K.-U., & Ramm, E., “Models and finite elements for thin-walled structures,” *Encyclopedia of Computational Mechanics*, Vol. 2: Solids, Structures and Coupled Problems, John Wiley & Sons, 2004, pp. 59–137, doi:10.1002/0470091355.ecm026.
- [23] Prabowo, A. R., Ridwan, R., Braun, M., Song, S., Ehlers, S., & Firdaus, N., “Comparative study of shell element formulations as NLFE parameters to forecast structural crashworthiness,” *Curved and Layered Structures*, vol. 10, 2023, Art. no. 20220217, doi:10.1515/cls-2022-0217.
- [24] Ahn, J. S., “A computationally efficient p-refinement finite element method approach for the fracture analysis of axially cracked pipes with composite patch reinforcement,” *Applied Sciences*, vol. 15, no. 5, p. 2711, 2025, doi:10.3390/app15052711.
- [25] Ye, J., Quan, G., Yun, X., Guo, X., & Chen, J., “An improved and robust finite element model for simulation of thin-walled steel bolted connections,” *Engineering Structures*, vol. 250, p. 113368, 2022, doi: 10.1016/j.engstruct.2021.113368.

- [26] Fu, M., Chen, J., Wang, B., & Wang, B., “An efficient strength evaluation method based on shell-fastener model for large hybrid joint structures of C/SiC composites,” *Materials*, vol. 17, no. 23, p. 6008, 2024, doi:10.3390/ma17236008.
- [27] Adkine, A. S., Overikar, G. P., & Surwase, S. S., “Modal analysis of engine supporting bracket using finite element analysis,” *International Journal of Advanced Engineering Research and Science*, vol. 4, no. 3, pp. 237–244, 2017, doi:10.22161/ijaers.4.3.9.
- [28] Gülbahçe, E., Yıldız, M., & Çelik, E., “Topology design and modal analysis of a jet engine bracket using finite element analysis,” *Applied Engineering Letters*, vol. 4, no. 3, pp. 102–105, 2019.
- [29] G. R. Liu and S. S. Quek, *The Finite Element Method: A Practical Course*, 2nd ed., Oxford, U.K.: Elsevier, 2013.
- [30] R. K. Roy, *A Primer on the Taguchi Method*, 2nd ed., Dearborn, MI, USA: Society of Manufacturing Engineers, 2010.
- [31] D. C. Montgomery, *Design and Analysis of Experiments*, 9th ed., Hoboken, NJ, USA: John Wiley & Sons, 2017.
- [32] P. J. Ross, *Taguchi Techniques for Quality Engineering*, 2nd ed., New York, NY, USA: McGraw-Hill, 1996.
- [33] J. Antony, *Design of Experiments for Engineers and Scientists*, Oxford, U.K.: Butterworth-Heinemann, 2003.
- [34] M. Işık et al., “Topology optimization and manufacturing of engine bracket using electron beam melting,” *Journal of Additive Manufacturing Technologies*, vol. 1, no. 3, p. 583, 2021, doi: 10.18416/JAMTECH.2111583.
- [35] F. Erdemir and M. T. Özkan, “Application of Taguchi method for optimization of design parameters in enhancement the robust of ‘C’ type snap-fits,” *Politeknik Dergisi*, vol. 25, no. 3, pp. 1385–1395, 2022, doi: 10.2339/politeknik.1076061.
- [36] F. F. Yusubov, “Wear studies on phenolic brake-pads using Taguchi technique,” *Tribology in Industry*, vol. 43, no. 3, pp. 489–499, 2021, doi: 10.24874/ti.1024.12.20.03.